Augmenting Flexibility: Mutual Inhibition Between Inhibitory Neurons Expands Functional Diversity

Belle Liu[1, *], Alexander James White[2, *, ✉], and Chung-Chuan Lo[2, 3, ✉]

[1] *Department of Physics, National Tsing Hua University, Hsinchu, Taiwan*

[2] *Institute of Systems Neuroscience, National Tsing Hua University, Hsinchu, Taiwan*

[3] *Brain Research Center, National Tsing Hua University, Hsinchu, Taiwan*

Abstract

One of the most intriguing observations of recurrent neural circuits is their flexibility. Seemingly, this flexibility extends far beyond the ability to learn, but includes the ability to use learned procedures to respond to novel situations. Here, we report that this flexibility arises from the synergistic interplay between recurrent mutual excitation and recurrent mutual inhibition. Specifically, we show that mutual inhibition is critical in expanding the functionality of the circuit, far beyond what feedback inhibition alone can accomplish. By taking advantage of dynamical systems theory and bifurcation analysis, we show mutual inhibition doubles the number of cusp bifurcations in the system in small neural circuits. As a concrete example, we build a simulation model of a class of functional motifs we call Coupled Recurrent inhibitory and Recurrent excitatory Loops (CRIRELs). These CRIRELs have the advantage of being multi-functional, performing a plethora of functions, including decisions, switches, toggles, central pattern generators, depending solely on the input type. We then use bifurcation theory to show how mutual inhibition gives rise to this broad repertoire of possible functions. Finally, we demonstrate how this trend also holds for larger networks, and how mutual inhibition greatly expands the amount of information a recurrent network can hold.

Introduction

Organisms often exhibit a vast range of behaviors, and these behaviors requires the neural network to perform different tasks. In light of this, an efficient design is for neural networks to be capable of flexibly switching

* Contributed equally to this work.

✉ Send Correspondence to Alexander White: ajw131@case.edu, or Chung-Chuan Lo: cclo@mx.nthu.edu

between various functions upon demand [1, 2, 3, 4, 5, 6, 7, 8, 9], instead of having each task be performed by a different network. [2, 10, 11, 9, 12]. This flexibility has indeed been observed experimentally[13, 14, 3, 15], but how this flexibility came to be remains a topic of investigation.

It has been hypothesized that a key component of this flexibility is the recurrent nature of neural connections [10, 16, 11]. Quite often the focus of the recurrent structures is on mutual excitation [17, 18, 19, 4, 20, 21] or feedback inhibition [22, 20, 23, 24, 25], and the role of mutual inhibition has not been well studied (the term "recurrent" has been used interchangeably across literature, see Fig. 1a for how it is defined in this study). However, there are several pieces of evidence suggesting that mutual inhibition plays a more crucial role than previously thought.

First of all, it has been widely reported that inhibitory neurons increase the variability of a network [26, 27, 28, 29], and supporting evidence from connectome studies revealed that recurrent connections are abundant [30, 31]. In particular, mutual inhibition is abundant and formed locally [32, 26], possibly performing local computations [33, 22]. Secondly, evident shows that there are functional differences between feedback and mutual inhibition. For example, feedback inhibition is composed of a interconnected pair of excitatory and inhibitory neuron, which balances the network [25, 34], allows networks to approximate arbitrary functions [16], and are useful in gain control. On the other hand, mutual inhibition increases the number of basin of attractions [4], allowing the network to perform functions such as winner-take-all decision [35, 36, 4, 37], oscillations [38, 11, 10], assosiative memory [39] and grid formation [40]. The wide variety of computations that mutual inhibition is capable of performing, along with connectome studies, all point to the idea the mutual inhibition is crucial in expanding a network's functional repertoire.

At last, we note that a network's functional capacity is not determined solely by the number of synapses [26, 41, 34, 42]. In particular, while each type of synapse increases the amount of potential computations a network can have, the network is not necessarily flexible if it cannot seamlessly transition between different functional modes. Whether the network is capable of easy transitions is highly dependent on the underlying bifurcation structure[43, 10]. Specifically, a previous theoretical study states that networks near complicated bifurcation structures are computationally useful [10], because only networks near a bifurcation have non-trivial dynamics [10, 16]. In short, one can control the specific operations a neuron can perform by controlling which bifurcations a circuit is near.

With this in mind, we hypothesize that mutual inhibition can increase the flexibility of a network by increasing the number of bifurcations the network is near. Specifically, it can subsume the functions originally present in the network, and introduce new functions on top of that. To further illustrate this argument, we

investigated the dynamics of a family of recurrent circuits we dubbed CRIREL (Coupled Recurrent Inhibition and Recurrent Excitation Loop). This type of structure is used across literature regarding a myriad of phenomena, such as decision making and deviance detection [44, 45].

To showcase the effect of different recurrent structures on a circuit's dynamics, we first conducted a series of statistical analysis. Based on these statistical results, we then delve into detailed a dynamical analysis of the CRIREL circuit. This shows how, by including mutual inhibition, even a small 4-neuron circuit is capable of a wide range of computations. Finally, we extend our study to a large random network and show that mutual inhibition is critical for increasing the entropy of its working memory state, which implies that mutual inhibition makes the dynamical landscape of a network more diverse.

Results

Effects of recurrent structures on complexity of circuit dynamics

We compared several circuit architectures (Fig. 1b) to distinguish between how different recurrent structures (Fig. 1a) contribute to a circuit's dynamics. The first metric we employed to characterize the diversity of circuit behavior was the number of equilibrium points. If the circuit contains multiple equilibrium points, it is more likely to lead to complex activity patterns in response to different inputs, an indication of the circuit's computational ability.

We begin with the CRIREL circuit, which contains all three recurrent structures, then remove these connections one at a time. Motif A contains all the recurrent structures indicated in Fig. 1a. Motif B doesn't contain mutual inhibition, and motif C doesn't have mutual excitation. In motif D and E, the feedback inhibition loop is broken – in motif D, feedback inhibition is removed, and in motif E, feedback excitation is removed. Motif F is a pure feedforward structure that was randomly chosen, and motif G is a feedforward structure that ultimately forms a loop on itself.

For each of the motifs, we performed a parameter sweep, where the synaptic weights of the circuit and bias currents were varied. A total of 18900 trials were ran. The protocol is designed so that it pushes the system in different directions in the phase space, ensuring that as much as possible is explored, which allows the algorithm to detect different equilibrium points. The firing rate sequence of the trial is then put though the Elbow method to judge the number of clusters that are formed, which correlates to the amount of stable equilibrium points in the system. Simply put, the Elbow method iterates through possible number of equilibrium points k, and performs K-means clustering on each iteration. The deviation of data points from its cluster's center of mass

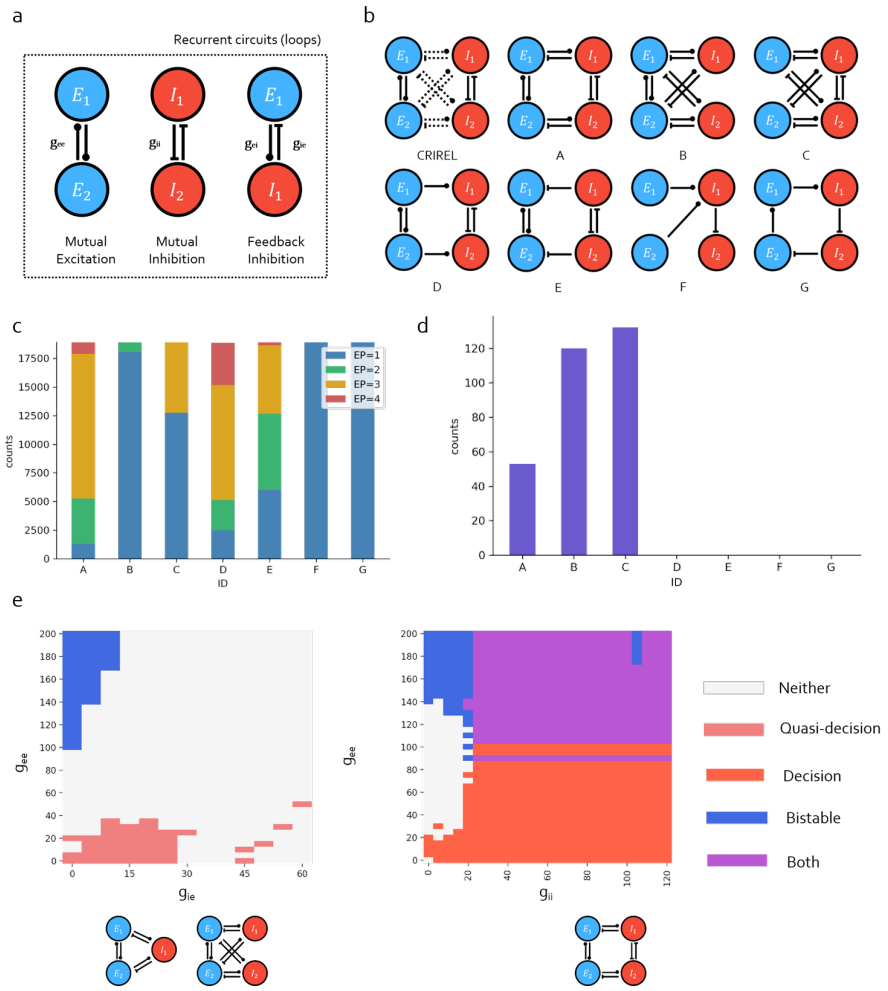

Figure 1: Motifs and statistical analysis of dynamical diversity. (a) Definition of the terms "recurrent" circuits, "mutual" excitation/inhibition and "feedback" inhibition used in this paper. Synaptic weights used in part of the results are assigned based on the pre- and post-synaptic neurons of said connection, hence there are four types of synaptic weights: excitatory-to-excitatory (g_{ee}), excitatory-to-inhibitory (g_{ei}), inhibitory-to-inhibitory (g_{ii}) and inhibitory-to-excitatory (g_{ie}). (b) The first motif labeled "CRIREL" is the definition of CRIREL circuits, where a mutual excitation and mutual inhibition loop is weakly coupled together in some manner. The rest of the motifs are indexed by alphabets in no particular order. Blue represents excitation neurons, and red inhibition. (c) Parameter sweep for equilibrium points in different motifs. For these motifs, we did a parameter sweep for each one of them and estimated the number of stable equilibrium points present within each parameter set. The relevant parameters here include g_{ee}, g_{ie}, g_{ii} and the underlying bias currents. In this graph, 1 equilibrium points is in blue (EP=1), 2 equilibrium points is green (EP=2), 3 is yellow (EP=3) and 4 is green (EP=4). (d) Parameter sweep for CPGs. For these motifs, the number of trials in which the motif becomes a central pattern generator (CPG) is plotted. The relevant parameters here include g_{ei} and g_{ie}. (e) A parameter sweep for motifs A and B. For motif B (left), the relevant parameters concerning quasi-decision making and switch are g_{ee} and g_{ie}. These determine the "strength" of the switch-like and decision-making functions, which are competing with each other since only one function is allowed be present at a time. Blue represents regions where the circuit can perform switching, coral-red represents decision making, and white represents no functions present. For motif A (right), the relevant parameters are g_{ee} and g_{ii}. g_{ie} is taken to be weak here. The purple region is the parameter regime in which the system can perform both functions simultaneously.

is calculated and summed (SSE, see Methods), where SSE typically decreases with the assumed number of clusters k. Whenever there is a large decrease in SSE as a function of k, it means that the algorithm has likely hit the correct number of clusters k.

The results show that motif A has the largest parameter regime in which the system not monostable, i.e. the number of equilibrium points exceed 1 (Fig. 1c; monostable in blue). Furthermore, motifs that have mutual inhibition (motifs A, C, D, E) have parameter sets with equilibrium point counts larger than two, while those with mutual excitation but not mutual inhibition has at most counts of two, and feedforward motifs have no bistability at all. In contrast, the presence or absence of feedback inhibition does not make such a large difference. For example, motifs A, D and E all have high numbers of equilibrium points, but D and E do not contain feedback inhibition while A does.

While the first metric shows the number of attractors in the network, it does not reveal whether other stable structures are possible within the network, such as oscillation given constant input. Therefore, the second metric we employed tested whether CPGs are present in the network. Our tests showed that the CPGs can be found in A, B and C – the ones that contain feedback inhibition (Fig. 1d).

In summary, we showed that mutual inhibition increases the number of attractors in the network, while feedback inhibition allows the network to oscillate when given constant input.

Functional differences between feedback and mutual inhibition

The statistical results indicate that mutual inhibition increases the dynamical states, but doesn't explain the mechanism behind it. Hence here we consider an explicit example that compares feedback inhibition with mutual inhibition – compares motif A with B, to be precise. We use the ability to simultaneously perform two functions: switch and decision making, as an indicator of the circuit's computational ability. That is, the circuit is in a parameter regime where both functions can be performed.

Motif B contains mutual excitation, which allows it to perform a switch-like function, where some brief positive current pulse can transfer the system to the ON state, and a negative pulse can turn it off. Motif B also has feedback inhibition, which skews the basin of attraction one way, therefore making one of the excitatory neuron fire faster than the other, performing a "quasi" decision making like function. (This is similar to decision making in the sense that one excitatory neuron will have a higher firing rate than the other; but it is crowned "quasi" because the firing rate difference isn't caused by a transition from one equilibrium point to another, as real decision making networks do.) However, these two functions cannot coexist within the circuit. This is due to the fact that one mutual connection structure, in this case mutual excitation, can only undergo one cusp

bifurcation. Therefore, either the mutual connection structure is strong, and the excitatory neurons are in sync with one another, which leads to switch; or the mutual connection is weak enough so that the excitatory neurons can be desynchronized by inhibition, which yields quasi-decision. This is seen in the parameter sweep in Fig. 1e, where we sweep over the synaptic weight parameter space (see Methods). As will be shown in more detail later, the combination of rudimentary functions such as switch and decision-making can create many more complicated and useful computations. Hence the inability to perform both functions simultaneously severely hinders the amount of functions the circuit can have.

If we add recurrent inhibition to the circuit, however, this problem can be resolved. Consider motif A, which has mutual excitation, feedback inhibition, as well as mutual inhibition. This second mutual connection structure adds another cusp bifurcation to the circuit, therefore the mutual excitation structure can be charged with performing the switch function, while mutual inhibition performs decision-making. This gives a large parameter regime in which motif A contains both functions simultaneously (Fig. 1e). Therefore, we see that the presence of mutual inhibition can add more functions to the underlying neural network.

Dynamics of CRIREL circuits

All of the statistical analysis above point to mutual inhibition being crucial in expanding the functional repertoire of a network. However, to have a better grasp on the functions CRIREL circuits actually bring about, we must look into its dynamics. To this end, we reduced the 4-dimensional CRIREL circuit into a 2-dimensional reduced model, with each of the recurrent circuits compressed into 1 dimension (see Supplementary). Conceptually, it can be understood as preserving the dimensions that are important to the dynamics of interest by considering the properties of the two mutual connections. Since mutual excitation tends to synchronize, the dimension of $e_1 - e_2$ is less important than $e_1 + e_2$ if the coupling is much weaker than the mutual connection strength, where e_i represents the firing rate of excitatory neuron i, which is denoted as E_i. On the other hand, mutual inhibition desynchronizes, therefore $i_1 + i_2$ is less important than $i_1 - i_2$ when the coupling is weak. Similarly, i_j represents the firing rate of inhibitory neuron j, which is denoted as I_j. Hence, by retaining the dimensions of $e_1 + e_2$ and $i_1 - i_2$ only, we can gain a geometrical understanding of how the system operates, which in turn sheds light on the potential computations recurrent circuits can perform (Fig. 2a).

The resulting reduced model is shown in Fig. 2b, where $\mathbf{E} = e_1 + e_2$ and $\mathbf{I} = i_1 - i_2$. The blue and red line represents the nullclines of $\mathbf{E}$ and $\mathbf{I}$ respectively. Note that both nullclines are of a cubic form, which is the normal form of a cusp bifurcation, thereby proving that mutual connections do indeed add cusp bifurcations to the circuit. Since there are two cubic functionss, we know that this system has a double-cusp bifurcation. There

are four free parameters in this reduced model, which comes from complicated nonlinear mappings of the original neuronal and bias current parameters. For physical intuition, a_1 and b_1 are nonlinear mappings of structural parameters of the neurons, such as capacitance or time constant or synaptic weights. a_2 and b_2 are mappings from the bias currents into the circuit. These parameters allow the cubic functions to change shape as well as translation, which gives rise to many different phase diagrams (Fig. 2c). These phase diagrams correspond to different "modes" of the circuit, in which it performs different functions. We will go over all of the functions we discovered below, but note that this is by no means a complete list of what the circuit is capable of doing.

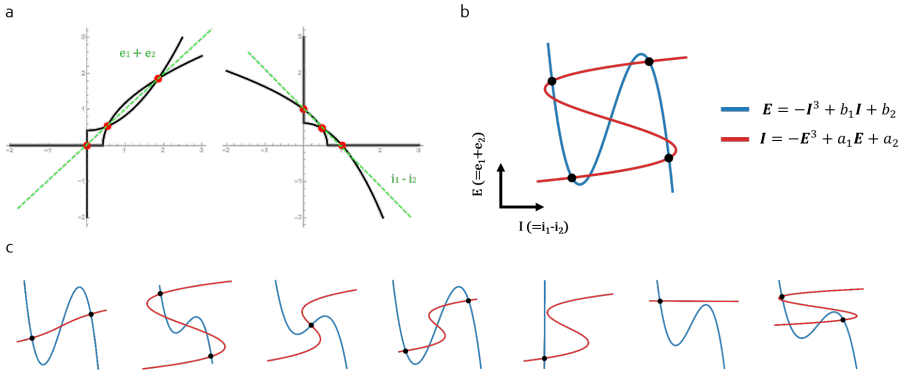

Figure 2: The reduced model of the CRIREL circuit. (a) When the two mutual excitation and inhibition loop are decoupled, their phase diagrams look like this respectively (excitation: left, inhibition: right). The black curves are nullclines and the red spots represent equilibrium points. The green dashed line shows the direction in which in interesting dynamics lie on (it is only approximate for the inhibitiory case). (b) When weakly coupled together, the CRIREL circuit can be reduced to two dimensions. The blue curve is the nullcline of the mutual excitation loop, red is the nullcline of mutual inhibition, and black dots are stable equilibria. (c) By adjusting the four parameters a_1, a_2, b_1 and b_2, the reduced model will change into different configurations, each of them corresponding to different functions.

Computational abilities of CRIREL circuits

The functions of CRIREL circuits include rudimentary ones that rely more heavily on mutual excitation, such as switch, toggle and synchronized CPG; it also includes ones in which computations are mainly performed in the mutual inhibition loop, such as decision-making and anti-synchronized CPG. Building from these concepts, we can also have computationally interesting functions, such as working memory, amplitude-based decision-making and timing-based decision-making.

Switch

We first demonstrate one of the simplest computations, which is a switch-like function. An intuitive understanding of switching is already described in previous sections. Here we demonstrate how to comprehend this

function geometrically using the reduced model. The reduced model for switch takes the form of Fig. 3c, where there are only two stable equilibrium points. The simulation begins at the equilibrium point where all the neurons are silent, i.e. the OFF state. When a brief positive current pulse is given to one or both of the excitatory neurons, the **E**-nullcline shifts upwards, annihilating the OFF state. Therefore the system transits to the remaining equilibrium point, i.e. the ON state, and remains there even as the input is removed and the **E**-nullcline returns to its original position. This means that the circuit will continue firing even in the absence of input. When a negative current pulse is applied, the opposite happens, and the system returns to the OFF state. This shows that the circuit is bistable. We see that the reduced model is consistent with the intuitive explanation given above. The simulation results are shown in Fig. 3a, and the shape of the reduced model in accordance with the evolution of the firing rate is shown in Fig. 3c.

Toggle and sCPG

A function that is similar to switch is toggle, except that it can be turned off by a positive current pulse instead of a negative pulse. This is shown graphically in Fig. 3b, which plots the voltage traces of one of the excitatory neurons (which are synchronized) and one of the inhibitory neurons. The first pulse causes the system to go to the ON state, and the firing rate of the inhibitory neurons are insufficient to inhibit the excitatory loop. However, when a second identical pulse enters the system, the firing rate of the excitatory loop increases, and concurrently the inhibitory loop. This extra push is enough for the inhibitory neurons to turn off the excitatory neurons, thus returning the whole system to inactivity.

Again, we can gain insight by examining the phase portrait of the system. The simple shifting mechanism of the switch-system no longer applies here. As shown in Fig. 3d, as the impulse current excites the excitatory loop and consequently the inhibition loop, the inhibitory response deepens, causing the inhibitory nullcline to change its shape. This in turns causes both the ON and OFF state to annihilate, and the system goes from 5 equilibrium points to one unstable spiral node. This means that for a brief amount of time, there exists a limit cycle and the system's state rotates. When the impulse input ends, the inhibitory system relaxes and the 5 equilibrium points return, but by that time the system is already trapped in the ON state. The second pulse repeats the process and rotates the system yet again, allowing it to return to the OFF state.

Interestingly, this implies that the circuit is also capable of sustaining periodic oscillations, that is, capable of becoming CPGs. Note that in Fig. 3e, if the impulse current is changed into a constant bias current, the system will repeat the process of toggling over and over again, thus undergoing a synchronized bursting behavior (sCPG for short). The phase diagram of sCPG is the limit-cycle mode shown in Fig. 3d.

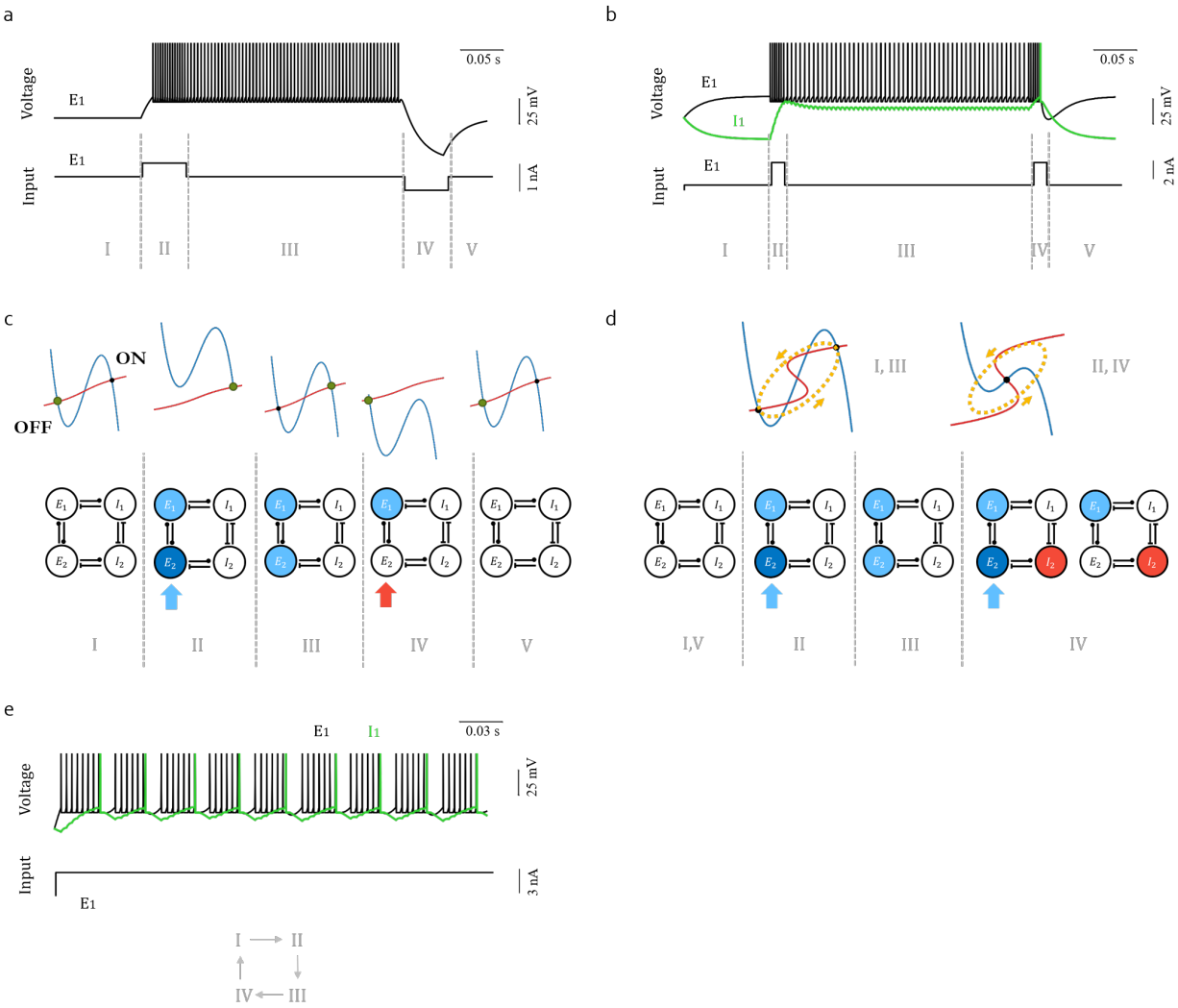

Figure 3: Switch, toggle and sCPG. (a) Switch voltage traces. Top row: the voltage trace of neuron E_1. Bottom row: the current input into E_1. When giving the neuron a positive current pulse, it turns on and remains on even when the input stops. When given a negative pulse, it turns off and stays off. (b) Toggle voltage traces. Top row: the voltage traces of E_1 (in black) and I_1 (in green). Bottom row: the current given to E_1. (c) Switch phase diagram. Top row: switch function phase diagram. The green dot represents the state of the system. Bottom row: Schematic diagram of the firing rates of each neuron during different time periods. Blue represents excitation, and red inhibition. The darker the color, the higher the activity. (d) Toggle phase diagram. Top row: toggle function phase diagram. Bottom row: Schematic diagram of the firing rates of each neuron during different time periods. (e) sCPG voltage traces. The rows are identical to those of (b). Here, however, the current into E1 is changed from pulses into a constant input. This causes the system to toggle over and over, thereby sustaining an oscillation. This is called the synchronized CPG since the activities of the excitatory neurons are synchronized with each other (as are the inhibitory with each other).

Decision making and aCPG

Switch, toggle and sCPG rely heavily on the dynamics of the mutual excitation loop. Decision making, on the other hand, is mainly due to mutual inhibition. For a decision network, when two inputs are injected into the neurons E_1 and E_2, the larger of the two inputs will "choose" their corresponding inhibitory neuron, thus preventing it from firing (Fig. 4a). Logically, this is the exact counterpart of the switch system, the difference

being that the nonlinearity now lies in the **I**-nullcline instead of the **E**-nullcline. While inputs shift the **E**-nullcline either up or down in the switch or toggle phase diagram, it shifts the inhibitory neuron either left or right in this case, hence forcing the system to decide between the two attractors. Geometrically, this corresponds to "rotating" the nullclines of the synchronized CPG by 90 degrees, as seen in Fig. 4c.

Similar to how toggle gives rise to synchronized CPGs, we can also change the current pulses to a constant bias here. This change will not yield anti-synchronized CPGs, since a constant bias would be reinforcing the system to stay within the same attractor. However, if we introduce time-scale seperation, e.g. mechanisms such as slow GABA synapses, calcium dynamics, and second-messenger systems, the circuit can oscillate. The phase diagram and simulation results are in Fig. 4b, d.

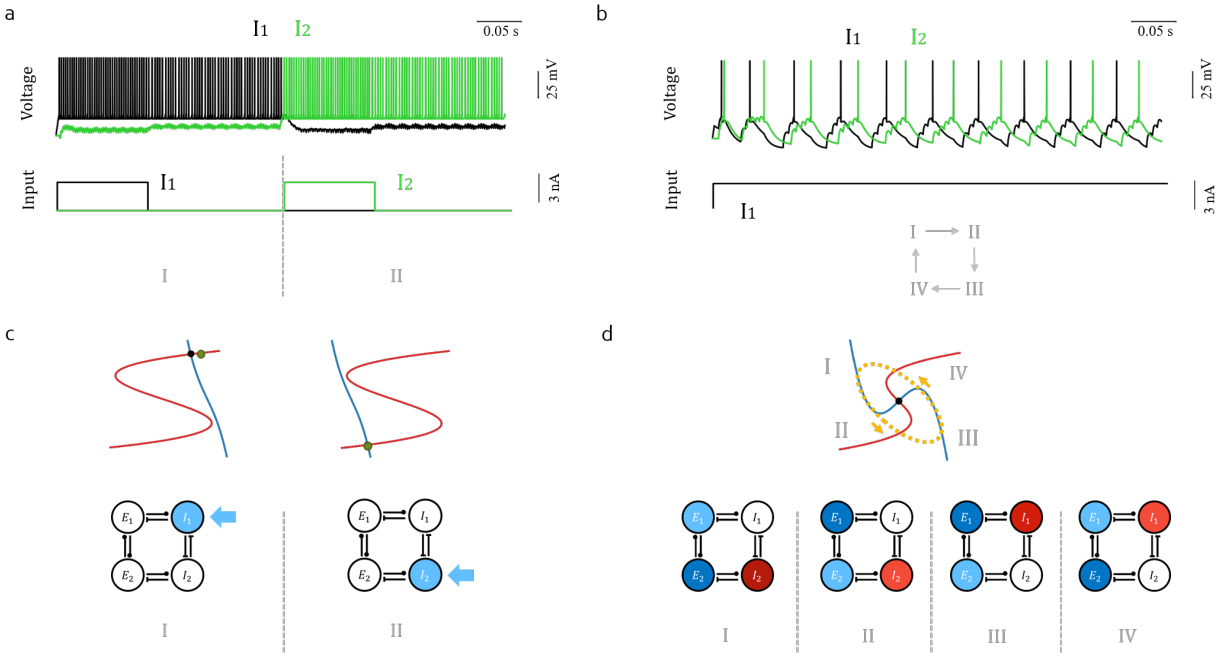

Figure 4: Decision making and aCPG. (a) Decision making voltage traces. Top row: the voltage traces of I_1 (in black) and I_2 (in green). Bottom row: is the current given to I_1 (in black) and I_2 (in green). When the input favors one of the neurons, that neuron will fire and suppress the other neuron. (b) aCPG voltage traces. The rows are identical to those of (a). Here, however, the current into I_1 and I_2 is changed from pulses into a constant input. Along with time scale separation, this causes the decision making process to renew itself again and again, creating an anti-synchronized CPG (the activities of E_1 and E_2 are anti-synchronized, as is I_2 and I_2). (c) Decision making phase diagram. (d) aCPG phase diagram.

Working memory

The situation described above complicates when the bistability of the excitatory sub-system is combined with decision making of the inhibitory sub-system. Since the ON state exists, this means that the decision can be remembered even after the input is withdrawn. As seen in Fig. 5, when receiving strong input, the excitation sub-system enters the ON state asymmetrically. One of the excitatory neurons will have higher firing rates, thus

allowing its neighboring inhibitory neuron to fire and inhibit the other one. Furthermore, the feedback inhibition strength is not strong enough to turn the excitatory sub-system off, thus the system "remembers" the input (Fig. 5a).

The analysis of this system is identical to those of Fig. 4c, except that there could be 4 equilibrium points, as shown in Fig. 5b. It can indeed be confirmed that this nullcline configuration is present in the full CRIREL system, where the inhibitory neurons can either be both on (i.e. (1, 1)), one on and one off (i.e. (1, 0) or (0, 1)) or both off (i.e. (0, 0)). Thus this system is capable of forming a working memory system with 2-bit memory. This is a perfect example of how simple functions such as decision making and switch can combine to yield a more interesting and useful function.

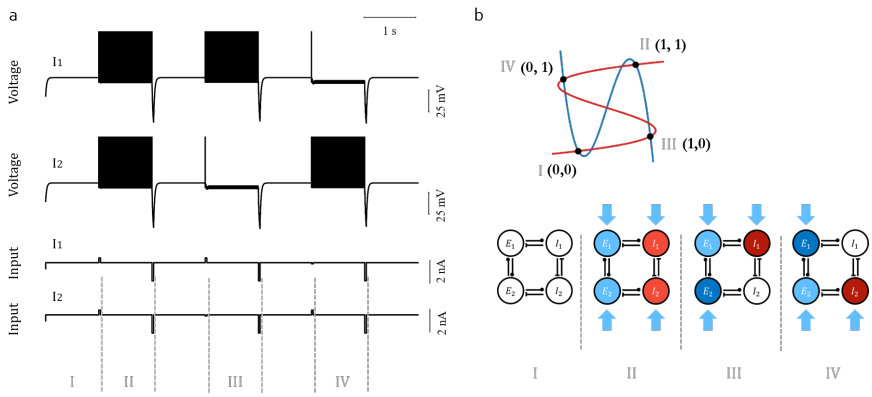

Figure 5: Working memory. (a) Voltage trace. This circuits stores a "two bit" signal in working memory, i.e. (1,1), (1,0), (0,1) and (0,0), corresponding to (I_1 on, I_2 on), (I_1 on, I_2 off), (I_1 off, I_2 on), (I_1 off, I_2 off). This can be seen in the top two rows of the graph, showing the voltage traces of I_1 and I_2. The bottom two rows are the inputs to the four neurons. This is because the system has four stable attractors, as shown in the phase diagram. Each attractor can thereby correspond to one state. (b) Phase diagram. Top row: phase diagram. Bottom row: Schematic diagram of the firing rates of each neuron during different time periods

Amplitude-based decisions

The capability of making decisions allows CRIRELs to be utilized in many different ways, including useful functions such as creating a safety net for hyperactivity. If we allow the CRIREL circuit to take on asymmetrical intrinsic and synaptic parameters (see Fig. 6c), the circuit can become a low-pass filter in terms of amplitudes, where small inputs are remembered by the circuit (working memory like), and larger ones terminate the bistability (toggle like). This computation is possible precisely due to the presence of asymmetries in the network. When one of the excitatory neurons receive a small input, since I_1 has stronger synaptic weights, I_1 will be chosen and thus inhibit I_2. However, when the input is sufficiently large, I_2 has smaller capacitance and time constants than I_1, and therefore will be excited faster than I_1, thus winning the decision. The feedback inhibition from I_1 is

weak, therefore when I_1 is chosen, it does not affect the network's bistability; however, the feedback inhibition from I_2 is strong, therefore whenever I_2 is chosen, the network shuts down. Hence the circuit serves as a gateway that filters out inputs that are too large, which is potentially useful for preventing epilepsy. Note that this model is a normative model, therefore we can also choose to put the asymmetries in the bias currents and not in the cell's membrane properties.

Timing-based decisions

Aside from making decisions based on the magnitude of the input, what is perhaps even more intriguing is making decisions based on the relative timing of inputs. Even a sub millisecond difference between the inputs is sufficient to bias the network to decide. Timing-based decisions can be accomplished if we allow sufficiently strong feedback inhibition, as we did in toggling. Under this condition, two modes are allowed: the coincidence detection mode (in a more engineering term, the AND mode) and the anti-coincidence detection mode (XOR mode). In the XOR mode, the network will chose whichever input came first, but will turn off completely if inputs arrive at the same time. In the AND mode, the network will only fire if the inputs arrive simultaneously.

Here, AND is controlled primarily by mutual excitation. The synaptic input is sufficient to turn the system on when both inputs arrive at the same time, but if there is a delay in the system then, the system will not fire. Conversely, the XOR system takes advantage of the toggle like dynamics, where it turns the system off if and only if both of the inputs arrive simultaneously. Otherwise, the inhibitory neurons do not fire with sufficient strength to turn the system off.

Memory in large network

So far, we have explicitly explained how mutual inhibition adds a cusp bifurcation to the circuit, which allows the circuit to perform various functions. We wish to extend this argument to large random networks, showing that an increase in mutual inhibition strength allows the network to have a wider variety of memory states.

The random network consists of 100 neurons, 75 excitatory and 25 inhibitory, where each connection has a 50 percent probability of being present (Fig. 7a). g_{ie} and g_{ii} are varied from 0 to approximately 30. For each parameter set, the excitatory neurons of the network are given random current pulses, and after the stimulation stops the network relaxes into a steady state. Since the stimulation is random, each time the steady state might be identical or different, and this is repeated for 100 times per parameter set. Each steady state is recorded as a "word", where different words represent different steady states (Fig. 7b; see Methods). The entropy for the distribution of the words across 100 trials, H_{word}, is calculated for the various parameter sets, which reflects how

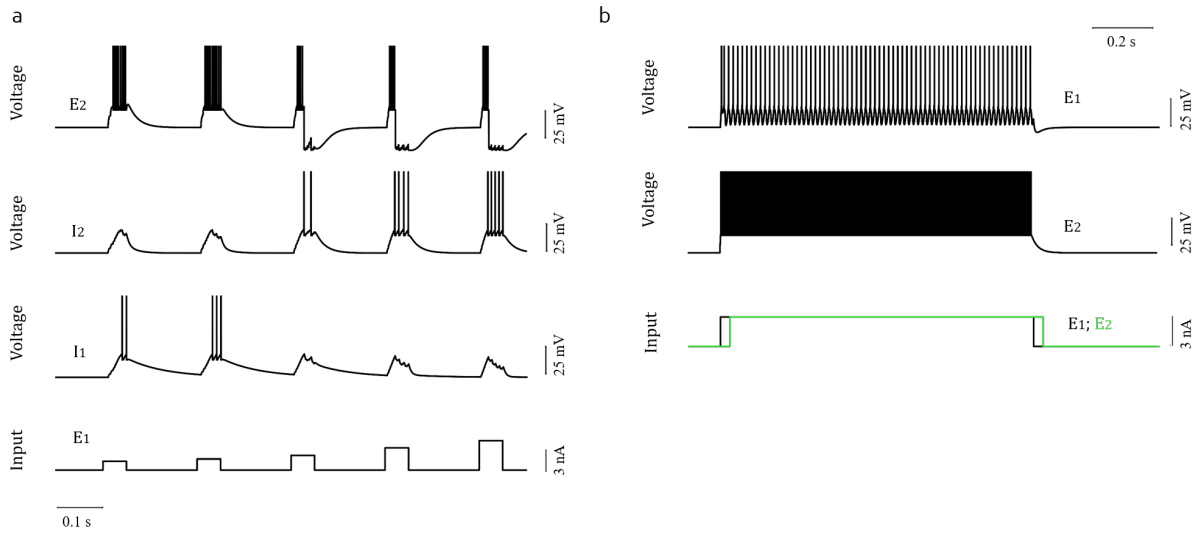

Figure 6: Amplitude-based and timing-based decision. (a) Amplitude-based-decisions. For this function, we used the motif 3-2447, which is asymmetrical, instead of motif A. The top three row shows the voltage traces of E_2, I_2 and I_1, and the bottom row shows the injected current into E_1. Here we inject neuron E_1 with different pulses of increasing amplitude. During the pulse both excitatory neurons turn on. However, because of the asymmetry between I_2 and I_1, low amplitude pulses I_2 turns on, but high amplitude pulses turn I_1 on. If I_1 turns on then it inhibits E_2, thereby shutting it off. Thus this circuit acts like a band pass filter, only letting low input signals through. (b) Timing-based decisions. Here we use motif A again. The top row is the voltage trace for E_1 (in black) and E_2 (in green). The bottom row is the input for E_2 (in black) and E_1 (in green). Here we have two input signals, one into E_1 and the other into E_2. E_1 occurs slightly before E_2. This small timing difference is enough to bias a winner takes all decision network and the network chooses I_1 and E_2.

diverse the steady states are (Fig. 7c).

Fig. 7c-d shows that for the same g_{ie} value, H_{word} increases as g_{ii} increases. To understand the reason behind this, we turn to two other entropy measures, H_{symbol} and H_{binary} (see Fig. 7b). Simply put, H_{symbol} measures how diverse the firing rate across population is, for a single trial. If the activities of all neurons are high, like the left graph of Fig. 7d, then there are not a lot of symbols available to form a word, hence H_{symbol} would be low and consequentially H_{word} as well. In Fig. 7c, it is shown that there is a regime of suitable g_{ii} to g_{ie} ratio where H_{symbol} is maximized. This trend is quite different from H_{word}, where it increases almost monotonically with g_{ii}. Therefore, an increase in the number of symbols is not the main mechanism behind what we observed in H_{word}.

Therefore, we used yet another method for calculating entropy, H_{binary}. Here, if a neuron fires, it's labeled as "1", while a silent neuron is labeled "0" (Fig. 7b). Each time the network relaxes into a steady state, it yields a distribution of 1s and 0s across the neuron population, and the entropy for that distribution is calculated. Essentially, if the neurons' firing rates are more "all or nothing" (or "winner takes all") – so that the ratio between the count of 1s and 0s are more equal – then H_{binary} will be higher. The higher H_{binary} becomes, the

lower the variety of words. And as shown in Fig. 7, H_{binary} is augmented as g_{ii} increases, which follows a similar trend to H_{word}.

To conclude, increasing g_{ii} increases the number of memory states the network contains. Consistent with how mutual inhibition introduces new bifurcations to the CRIREL circuit, mutual inhibition in a large network also complicates its dynamics and yields a more computationally useful product. The large network is also capable of performing other functions found in the CRIREL circuit (see Supplementary).

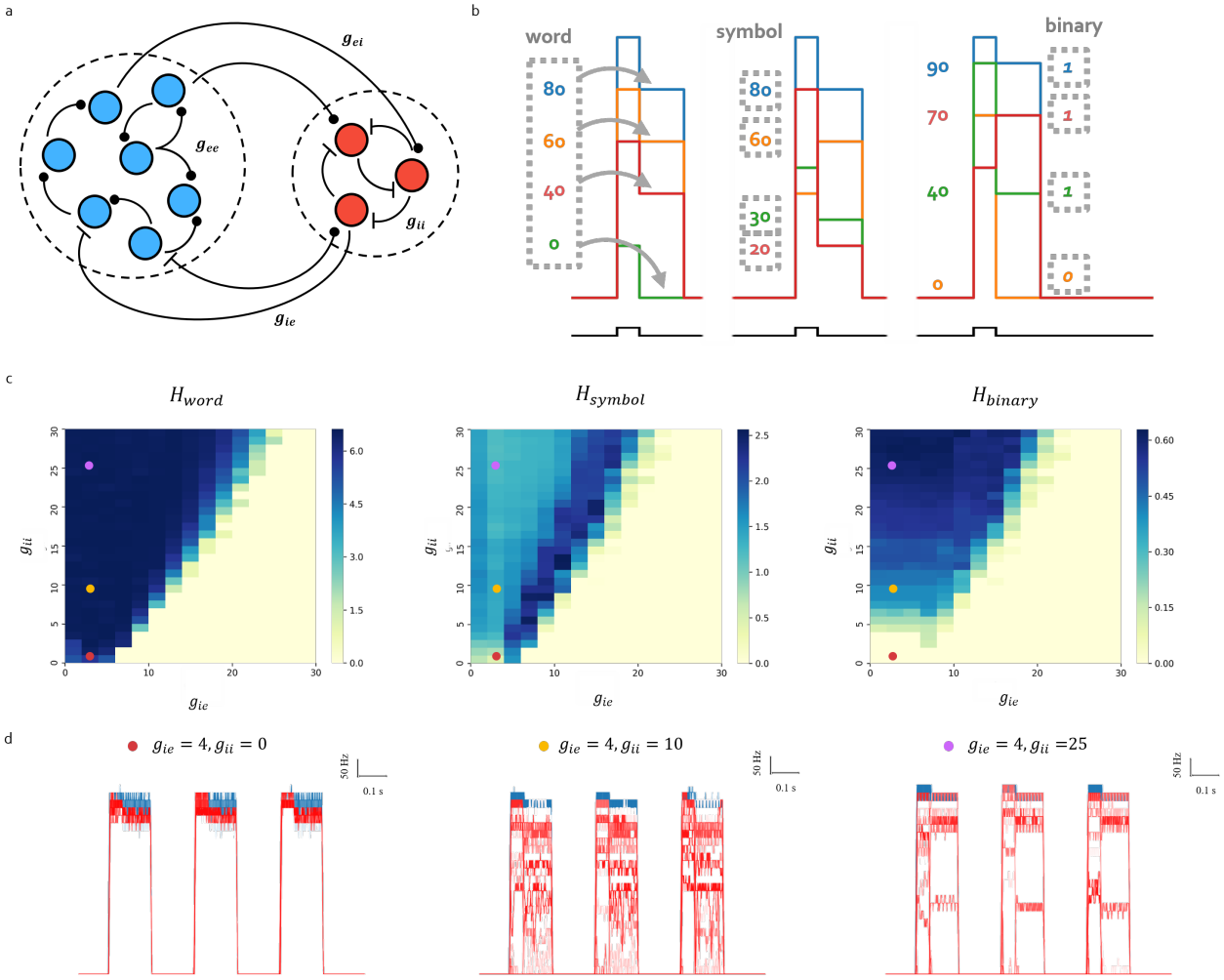

Figure 7: Memory in large network. (a) Schematic diagram of large random network. (b) Schematic diagram of how entropy is calculated. Each line represents the firing rate of a neuron, and the firing rate of the neuron population is defined as a "word". The words across 100 trials forms a probability mass function, which is used to calculate H_{word}. The word itself is also a probability mass function for different firing rates, which also has an associated entropy. The trial-average of this entropy is called H_{symbol}. Alternatively, each neuron can be labeled as on (1) or off (0), and the entropy associated with this is called H_{binary}. (c) From left to right: H_{word}, H_{symbol}, H_{binary} for different g_{ii} and g_{ie}. (d) Firing rate traces for neurons across 3 trials, with different synaptic weights. Blue traces represent excitatory neurons, and red traces inhibitory neurons. From left to right: increasing g_{ii}.

Discussion

In this study, we showed that mutual inhibition between inhibitory neurons increases the flexibility of small neural circuits using a mixture of bifurcation theory and statistical analysis. We began by showing that small motifs with mutual inhibition contains more unique states. We then showed a specific example of why this is the case, by using the functions switch and decision making. Based on that, we proposed a reduced model of the CRIREL circuit, which illustrated mechanistically why mutual inhibition is critical in expanding functionality and endowing brain networks flexibility. Finally, we extended the argument of the importance of mutual inhibition from small circuits to large networks, where we demonstrated that the number of unique memory states increases with mutual inhibition strength.

Connectome studies

Connections between inhibitory neurons has been shown in many different contexts [32, 22, 26, 24, 23, 46]. The importance of mutual inhibition is clearer as it becomes easier to tease out fine-scale connectivity in nervous systems. We have shown computationally that these types of connections are useful and perform a unique role in computational processing by expanding the number of computational states a network has. As we showed, mutual inhibition is important because it adds cusp bifurcations into the dynamics of the network. This could help explain why neural circuits contain local inhibitory connections. Specifically, the cusp bifurcation is well known in explaining the dynamics of decision networks.[10, 35, 36, 4, 37]. Specifically, the additional cusp bifurcations help explains the increase number of equilibrium states, as each cusp bifurcation embeds additional basins of attraction into the network [10] .

Cusp bifurcations and mutual inhibition

These results are in line with studies that have shown that there is an increase in variability when the connection strength of inhibition is increased[26, 44]. Moreover, we showed that increases in g_{ii} is more responsible for the increase in steady states than g_{ie}. Again, this tracks with the presence of a multiple cusp bifurcation. Furthermore, as the large network simulations showed, for each inhibitory neuron with all-to-all inhibitory connections added there is an additional cusp bifurcation. This doubles the number of unique combinations of states the network can perform. While cusp bifurcations help explain the dynamics of decision networks, other studies have shown that networks that are near bifurcations are capable of more functions beyond simple decisions [10, 16].

Co-existence of functions

Furthermore, by taking advantage of the multiple unique cusp bifurcations that mutual inhibition provides, we can embed multiple functions into a single network such as switch, toggling, decision making, CPG, and chaos. Much like many studies on flexibility [11, 9, 38] we can switch between these functionality easily, with either changes in synaptic weights constant inputs or changes in bias current. Again, we showed that while many of these functions can exist without mutual inhibition; they cannot coexist with other functions.

Hopf bifurcations and feedback inhibition

However, we focused primarily on the effect of recurrent inhibitory loops, specifically mutual inhibition. This bidirectional symmetry allows the network to operate near a cusp bifurcation. However, this underplays the existence and usefulness of other potential bifurcations. For example, in the feedback inhibition case with less symmetry imposed on the network, the network is closer to a single equilibrium point with positive complex eigenvalues. This strongly suggests these networks are near multi-Hopf bifurcations as well. Moreover, feedback inhibition is clearly important to functionality of networks [20, 16, 22, 26, 32]), even though we did not focus on feedback inhibition in this study. These types of connections also can cause complex positive eigenvalues, especially for smaller values of g_{ii}. In addition, the existence of toggle and CPGs strongly imply that feedback and mutual inhibition add to functional flexibility, not subtract from it. It would be interesting to examine a reduction technique for slightly larger neural networks that includes the multiple-Hopf bifurcations rather than just the multi-cusp bifurcation.

Gap junction

Another area that can be extended to is examining the effects of gap junctions on the network. Some have found that mutual inhibition and gap junctions tend to coexist in some circuits [32]. It has been shown that gap junctions have a tendency to average out the winner-take-all aspect of the decisions [35, 36, 4, 37]. It would be interesting to investigate the effects of gap junctions on CRIREL type circuits.

Also we have mostly overlooked plastic synapses. Yet there has been much work showing that this is a important component in network functionality[5, 42, 39, 41, 38]. Moreover there has been recent work that shows how synaptic depression can desegregate different cusp bifurcations by weakening the strong synaptic effects between recurrent excitatory loops [34]. Furthermore, by using plastic synapses, one can construct networks that are both balanced, and near bifurcations[16]. Investigating how learning and plastic synapse can work synergistic with mutual inhibition is a key goal in our future work.

Network control

A final direction for future work is to examine the best way to control networks with mutual inhibition. Several studies have suggested that networks near bifurcations are computationally useful [10, 16]. Some studies use balanced inhibition to tune the network to be useful [16]. Here, we wonder if this process can be used to control networks with mutual inhibition. If mutual inhibition is removed, are these networks still computationally useful?

To conclude, we have shown that mutual inhibition is key in expanding the functionality of the network. This is possible because mutual inhibition expands the number of cusp bifurcations in a network. Ultimately this helps elucidate why neural circuits in the brain are so flexible in their operation and are capable of such rich dynamics.

Methods

Spiking neural model and synaptic model

Each individual neuron was modeled as a leaky integrate-and-fire neuron:

$$C_m \frac{dV}{dt} = -\frac{C_m}{\tau}(V - E_L) + \sum I_j^{syn}(t) \tag{1}$$

$$\text{When } V > V_{Th} \text{ then } V \to V_{reset},\ t \to t + t_{re} \tag{2}$$

where C_m is the capacitance, V the membrane potential, τ is the time constant, E_L the reversal potential, and I_j^{syn} the current from the jth presynaptic neuron. The simulations were ran on flysim [33].

Excitation is modeled by as an exponentially decaying AMPA receptor, while inhibition is modeled as and exponentially decaying GABA receptor. More precisely, we have have excitatory and inhibitory current given by

$$I_{Ampa}(t) = g_{Ampa} s_{Ampa}(t)(V - E_{Ampa})$$

$$\tau_{Ampa} \frac{ds_{Ampa}}{dt} = -s + \sum_{t_{spike}} \delta(t_{spike} - t)$$

$$I_{Gaba}(t) = g_{Gaba} s_{Gaba}(t)(V - E_{Gaba})$$

$$\tau_{Gaba} \frac{ds_{Gaba}}{dt} = -s + \sum_{t_{spike}} \delta(t_{spike} - t)$$

Here, I is the current of the receptor, V is the post synaptic current, E is the driving potential of the receptor, g is the conductance of the receptor, s is the gating variable for the receptor ion channel. Furthermore, s is governed by a linear ODE with time constant τ, and is forced by a sum of dirac delta impulses $\sum_{t_{spike}} \delta(t_{spike} - t)$

where t_{spike} is the timing of presynaptic spikes. It is important to note that $g_{ee} = g_{Ampa}$ when both pre and post synaptic neurons are excitatory and $g_{ei} = g_{Ampa}$ when presynaptic neuron is excitatiory and postsynaptic neuron is inhibitory. Likewise, $g_{ii} = g_{Gaba}$ when both pre and post synaptic neurons are inhibitory and $g_{ie} = g_{Gaba}$ when presynaptic neuron is inhibitory and postsynaptic neuron is exicatitory.

Spiking Neural Model Parameters			
Parameter	Value	Parameter	Value
C_m	0.5	τ_{AMPA}	2
τ	20	V_{AMPA}	0
E_L	-70	τ_{GABA}	5
V_{reset}	-55	V_{GABA}	-90
V_{Th}	-50		

Table 1: Parameters for neuronal model and synaptic model.

Equilibrium points in microcircuits

It is conceivable that the functional repertoire of a motif is correlated to the abundance of its dynamical states. Here, we employ a statistical approach that provides us an estimate of the number of equilibrium points in relevant parameter space. We compared motifs that are specifically chosen to highlight the presence or absence recurrent loops, along with some randomly chosen feedforward motifs. These motifs are shown in Fig. 1b.

Parameter Space

To lower dimensionality in parameters, we constrained synaptic weights with the same type of pre-synaptic and post-synaptic neuron to have the same value (see Fig. 1a). Thus we have four types of synaptic weights: excitatory-to-excitatory (g_{EE}), excitatory-to-inhibitory (g_{EI}), inhibitory-to-inhibitory (g_{II}) and inhibitory-to-excitatory (g_{IE}). For each motif, we ran simulations over 18900 trials, where each trial has a different synaptic weight parameter set g_{EE}, g_{IE}, g_{II}.

Aside from synaptic weights, we also iterated through different underlying bias currents in the neurons. The bias currents adjust the threshold for firing, allowing inhibitory neurons to fire in the absent of excitatory input. This ensures that we capture the dynamic states produced by the inhibitory neurons. For each trial, a brief injected current goes into different pairs of neurons, for example one trial would stimulate E_1 only, and another would stimulate E_1 and I_1 simultaneously. This is ran through all possible pairs. The amplitude of the

stimulus changes as well. Both stimulating different pairs as well as varying the stimulus amplitude ensures a wider exploration of the parameter space, thereby allowing us to find more attractors. Each brief pulse of positive stimulation is separated by a negative reset signal. These are shown in Supplementary. Note that this method may not capture all of the equilibrium points present, nor will it be able to detect other stable structures such as limit cycles.

Clustering

To analyze the amount of attractors present in each trial, we look at the firing rate trace of the motif across the four-dimension space (e_1, e_2, i_1, i_2). We used the elbow method to obtain the amount of clusters in the firing rate trace of the trial. The elbow method detects the number of clusters by iterating through possible guesses and performing K-means clustering, and then evaluating each guess with its standard deviation, which is $SSE = \sum_{i=1}^{k} \sqrt{\frac{\sum_{j=1}^{N_i}(r_{ij}-\bar{r_i})^2}{N_i-1}}$. By plotting the standard deviation of several k values together, we see that sometimes the plot has a sharp drop, which is cleverly termed "the elbow" (see Supplementary). Such a sharp drop usually indicates that the number of clusters assigned has hit the correct amount. If no elbows are present, then the data set most likely only has one cluster. A criteria is needed to determine "how sharp" a drop can be considered an elbow, and this criteria is set so that the slope of the "arm" must be seven times the slope of the "forearm".

We purposely neglected the transient activities 100ms after a positive stimulation pulse or a negative reset signal in order to neglect "fake" clusters (i.e. clusters that are present, but aren't true attractors). Finally, the total number of equilibrium points in 18900 trials are calculated for each motif for comparison.

CPG in microcircuits

For CPGs, the parameter space was scanned across suitable values of g_{ie} and g_{ei}. The interspike interval (ISI) for each trial was calculated, and rounded to the nearest 0.001 (s). Since there is no noise in the system, the periodic firing of a neuron being driven by a constant current has a near perfect period (where the slight differences were accounted for by the rounding procedure), and thus the ISI would consist of one single value. For CPGs, the ISI would contain two or more values. The counts for trials with CPGs were calculated for each motif.

Decision Making and Bistability

To lower the dimensionality of the parameter space, again we constrained synaptic weights with the same type of pre-synaptic and post-synaptic neuron to have the same value. For bistability, since it happens within the excitatory subsystem, the most crucial synaptic weight is g_{EE}. For decision making in feedback inhibitory networks, the important synaptic weight is g_{IE}, since strong g_{IE} allows the circuit to turn off the unfavorable excitatory neuron. For decision making in mutual inhibitory networks, the key synaptic weight is g_{II}. Therefore, for the purpose of this analysis, we will hold g_{EI} constant and sweep through relevant parameter regimes of g_{EE}, g_{IE} and g_{II}.

For each point (g_{EE}, g_{IE}, g_{II}) in the parameter space, two trials with different input protocols are given to the network. The bistable protocol gives a 100 ms positive pulse to one of the excitatory neurons, resets the circuit using a strong negative pulse, and repeats this process for all of the excitatory neurons present within the network (see Supplementary). If the network is capable of bistability, then the pulse to one of the excitatory neurons should be able to turn the network to the ON state and remain there until the resetting pulse comes in. The decision protocol iterates through all possible pairs of excitatory neurons, where for each time period each pair is given an asymmetrical input (see Supplementary). If the network decides, then there will be a difference in firing rate between a pair of neurons at that time period. We test for two different pairs: the pair of excitatory neurons – corresponding to quasi-decision, and the pair of inhibitory neurons – corresponding to decision. Each point (EE, IE, II) will be capable of either bistability, quasi-decision, decision, both, or none. The results are then drawn into a heat map, where broader regions of "both functions present" means that it is more possible for the two functions to co-exist.

Dynamical analysis

The derivation of the reduced model is given in the Supplementary. The reduced model allows us to conceptually understand what is occurring dynamically in the spiking neural network. Furthermore, the intuition gained from the reduced model is invaluable, as any function found in the reduced model can also be found in the spiking model for an appropriate set of parameters. This is a consequence of topological equivalence. Note that this does *not* work in the converse direction, meaning there could be functions in the spiking model that are not in the reduced model.

As a broad overview, we first begin by showing that the mutual excitatory loop and the mutual inhibitory loop each have a cusp bifurcation. To contrast this, we also showed that feedback inhibition cannot undergo a cusp bifurcation. Next, we coupled the two circuits together, and show that both cusps are maintained. Finally,

we worked out the reduced model's simple cubic form.

CRIREL function simulations

While the reduced model is general for the whole class of CRIREL circuits, the results we've shown are simulated on one particular circuit (motif A in Fig. 1b, labeled as 3-3435), with the exception of amplitude-based decision, which is simulated on motif 3-2447 (see Supplementary).

Large random network

To construct the large network, we used 100 LIF neurons with the same membrane parameters as the microcircuits. The excitatory population had 75 neurons, while the inhibitory population had 25 neurons. The parameters for connection probability and synaptic weights are given in Supplementary materials.

Each excitatory neuron was given a random 500 ms pulse with an amplitude drawn from an normal distribution $N(3, 3)$ in addition to an underlying bias current of -5 nA. After the pulse ends, we waited for an extra 1 s before giving a reset signal of -20 nA to the excitatory neurons. Through this protocol, if the network is capable of sustaining memory, then it will settle into a random attractor after the pulse is removed. Three different types of entropy are calculated to analyze the variety of memory states in the network.

Entropy

For a discrete random variable X, where there are n potential outcomes $x_i, ...x_n$ with associated probability $P(x_1), ...P(x_n)$, its entropy is

$$H(X) = -\Sigma_{i=1}^{n} P(x_i) log P(x_i) \tag{3}$$

Entropy of words, H_{word}

After the pulse is turned off and before the reset signal arrives, each neuron i will have a different time-averaged firing rate $\bar{r_i} = \langle r_i \rangle_t$, which represents the "state" the neuron is in for that particular attractor. Together, these firing rates can form a sequence, i.e. $r_1, r_2, r_3, ...r_1 00$, which we call a "word". Each trial will produce one such word. If the memory network has multiple attractors, then the variation of words would be large, and the entropy resulting from such a distribution of words, H_{word}, would be large.

When calculating the entropy, what we actually used is the quotient of $\bar{r_i}$ over 20. This is similar to grouping the firing rate into different bins, where the firing rates within the same bin is assumed to carry the same amount of information.

Entropy of symbols, H_{symbol}

A word $r_1, r_2, r_3, ...r_100$ itself is a distribution of firing rates. The entropy of this distribution is called H_{symbol}, which reflects how widely distributed these firing rates are.

Entropy of binary symbols, H_{binary}

Instead of representing each neuron by its firing rate, we instead observe whether the neuron fires or not. If it fires, the neuron is given a label $l_i = 1$, and $l_i = 0$ otherwise. This again forms a distribution across the neuron population, $l_1, l_2, l_3, ...l_100$, and its associated entropy is called H_{binary}.

References

[1] Krishna V. Shenoy, Matthew T. Kaufman, Maneesh Sahani, and Mark M. Churchland. A dynamical systems view of motor preparation: Implications for neural prosthetic system design. *Progress in brain research*, 192:33–58, 2011.

[2] Guangyu Robert Yang, Madhura R. Joglekar, H. Francis Song, William T. Newsome, and Xiao-Jing Wang. Task representations in neural networks trained to perform many cognitive tasks. *Nature Neuroscience*, 22(2):297–306, February 2019.

[3] Christian K. Machens, Ranulfo Romo, and Carlos D. Brody. Flexible Control of Mutual Inhibition: A Neural Model of Two-Interval Discrimination. *Science*, 307(5712):1121–1124, February 2005.

[4] Xiao-Jing Wang. Decision Making in Recurrent Neuronal Circuits. *Neuron*, 60(2):215–234, October 2008.

[5] Alain Destexhe and Eve Marder. Plasticity in single neuron and circuit computations. *Nature*, 431:789–795, October 2004.

[6] Eve Marder and Vatsala Thirumalai. Cellular, synaptic and network effects of neuromodulation. *Neural Netw*, 15(4-6):479–493, July 2002.

[7] Ronald M. Harris-Warrick and Eve Marder. Modulation of neural networks for behavior. *Annual Review of Neuroscience*, 14:39–57, 1991.

[8] Cornelia I. Bargmann. Beyond the connectome: how neuromodulators shape neural circuits. *Bioessays*, 34(6):458–465, June 2012.

[9] David N. Lyttle, Jeffrey P. Gill, Kendrick M. Shaw, Peter J. Thomas, and Hillel J. Chiel. Robustness, flexibility, and sensitivity in a multifunctional motor control model. 111(1):25–47.

[10] Frank C. Hoppensteadt and Eugene M. Izhikevich. Local Analysis of Weakly Connected Maps. In Frank C. Hoppensteadt and Eugene M. Izhikevich, editors, *Weakly Connected Neural Networks*, Applied Mathematical Sciences, pages 209–218. Springer New York, New York, NY, 1997.

[11] Randall D. Beer. On the Dynamics of Small Continuous-Time Recurrent Neural Networks, 1995.

[12] H. Francis Song, Guangyu R. Yang, and Xiao-Jing Wang. Training Excitatory-Inhibitory Recurrent Neural Networks for Cognitive Tasks: A Simple and Flexible Framework. *PLOS Computational Biology*, 12(2):e1004792, February 2016.

[13] Mark M. Churchland, John P. Cunningham, Matthew T. Kaufman, Stephen I. Ryu, and Krishna V. Shenoy. Cortical preparatory activity: representation of movement or first cog in a dynamical machine? *Neuron*, 68(3):387–400, November 2010.

[14] Eve Marder and Adam L. Taylor. Multiple models to capture the variability in biological neurons and networks. *Nat. Neurosci.*, 14(2):133–138, February 2011.

[15] Woodrow L. Shew, Hongdian Yang, Shan Yu, Rajarshi Roy, and Dietmar Plenz. Information Capacity and Transmission Are Maximized in Balanced Cortical Networks with Neuronal Avalanches. *Journal of Neuroscience*, 31(1):55–63, January 2011.

[16] Guillaume Hennequin, Tim P. Vogels, and Wulfram Gerstner. Optimal Control of Transient Dynamics in Balanced Networks Supports Generation of Complex Movements. *Neuron*, 82(6):1394–1406, June 2014.

[17] Ashok Litwin-Kumar and Brent Doiron. Slow dynamics and high variability in balanced cortical networks with clustered connections. *Nature Neuroscience*, 15(11):1498–1505, November 2012.

[18] Yangfan Peng, Federico J. Barreda Tomás, Constantin Klisch, Imre Vida, and Jörg R. P. Geiger. Layer-specific organization of local excitatory and inhibitory synaptic connectivity in the rat presubiculum. 27(4):2435–2452.

[19] Stephanie C Seeman, Luke Campagnola, Pasha A Davoudian, Alex Hoggarth, Travis A Hage, Alice Bosma-Moody, Christopher A Baker, Jung Hoon Lee, Stefan Mihalas, Corinne Teeter, Andrew L Ko, Jeffrey G Ojemann, Ryder P Gwinn, Daniel L Silbergeld, Charles Cobbs, John Phillips, Ed Lein, Gabe Murphy,

Christof Koch, Hongkui Zeng, and Tim Jarsky. Sparse recurrent excitatory connectivity in the microcircuit of the adult mouse and human cortex. 7:e37349.

[20] Carl Holmgren, Tibor Harkany, Björn Svennenfors, and Yuri Zilberter. Pyramidal cell communication within local networks in layer 2/3 of rat neocortex. 551:139–153.

[21] R. J. Douglas, C. Koch, M. Mahowald, K. A. Martin, and H. H. Suarez. Recurrent excitation in neocortical circuits. 269(5226):981–985.

[22] Jianing Yu, Hang Hu, Ariel Agmon, and Karel Svoboda. Recruitment of GABAergic interneurons in the barrel cortex during active tactile behavior. 104(2):412–427.e4.

[23] Daniel Durstewitz, Jeremy K. Seamans, and Terrence J. Sejnowski. Neurocomputational models of working memory. 3(11):1184–1191.

[24] Katie A. Ferguson and Jessica A. Cardin. Mechanisms underlying gain modulation in the cortex. 21(2):80–92.

[25] Lotte J Herstel and Corette J Wierenga. Network control through coordinated inhibition. *Current Opinion in Neurobiology*, 67:34–41, April 2021.

[26] Netta Haroush and Shimon Marom. Inhibition increases response variability and reduces stimulus discrimination in random networks of cortical neurons. 9(1):4969.

[27] György Buzsáki and Xiao-Jing Wang. Mechanisms of Gamma Oscillations. *Annual Review of Neuroscience*, 35(1):203–225, June 2012.

[28] Yehezkel Ben-Ari. Excitatory actions of gaba during development: the nature of the nurture. *Nature Reviews Neuroscience*, 3(9):728–739, September 2002.

[29] Marla B. Feller. Spontaneous Correlated Activity in Developing Neural Circuits. *Neuron*, 22(4):653–656, April 1999.

[30] Olaf Sporns and Rolf Kötter. Motifs in Brain Networks. *PLoS Biol*, 2(11), November 2004.

[31] Rodney J. Douglas and Kevan A. C. Martin. Recurrent neuronal circuits in the neocortex. *Curr. Biol.*, 17(13):R496–500, July 2007.

[32] Claudia Espinoza, Segundo Jose Guzman, Xiaomin Zhang, and Peter Jonas. Parvalbumin + interneurons obey unique connectivity rules and establish a powerful lateral-inhibition microcircuit in dentate gyrus. 9(1):4605.

[33] Yu-Chi Huang, Cheng-Te Wang, Ta-Shun Su, Kuo-Wei Kao, Yen-Jen Lin, Chao-Chun Chuang, Ann-Shyn Chiang, and Chung-Chuan Lo. A Single-Cell Level and Connectome-Derived Computational Model of the Drosophila Brain. 2018.

[34] Gianluigi Mongillo, Simon Rumpel, and Yonatan Loewenstein. Inhibitory connectivity defines the realm of excitatory plasticity. *Nature Neuroscience*, 21(10):1463–1470, October 2018.

[35] Cheng-Te Wang, Chung-Ting Lee, Xiao-Jing Wang, and Chung-Chuan Lo. Top-down modulation on perceptual decision with balanced inhibition through feedforward and feedback inhibitory neurons. *PLoS ONE*, 8(4):e62379, 2013.

[36] Chung-Chuan Lo and Xiao-Jing Wang. Cortico–basal ganglia circuit mechanism for a decision threshold in reaction time tasks. *Nature Neuroscience*, 9(7):956–963, July 2006.

[37] Kong-Fatt Wong and Xiao-Jing Wang. A Recurrent Network Mechanism of Time Integration in Perceptual Decisions. *J. Neurosci.*, 26(4):1314–1328, January 2006.

[38] Eve Marder, Marie L. Goeritz, and Adriane G. Otopalik. ROBUST CIRCUIT RHYTHMS IN SMALL CIRCUITS ARISE FROM VARIABLE CIRCUIT COMPONENTS AND MECHANISMS. *Curr Opin Neurobiol*, 31:156–163, April 2015.

[39] J. J. Hopfield. Neural networks and physical systems with emergent collective computational abilities. 79(8):2554–2558.

[40] Jonathan J. Couey, Aree Witoelar, Sheng-Jia Zhang, Kang Zheng, Jing Ye, Benjamin Dunn, Rafal Czajkowski, May-Britt Moser, Edvard I. Moser, Yasser Roudi, and Menno P. Witter. Recurrent inhibitory circuitry as a mechanism for grid formation. *Nat. Neurosci.*, 16(3):318–324, March 2013.

[41] Frank C. Hoppensteadt and Eugene M. Izhikevich. Local Analysis of Singularly Perturbed WCNNs. In Frank C. Hoppensteadt and Eugene M. Izhikevich, editors, *Weakly Connected Neural Networks*, Applied Mathematical Sciences, pages 189–207. Springer New York, New York, NY, 1997.

[42] Bolun Chen and Paul Miller. Attractor-state itinerancy in neural circuits with synaptic depression. *The Journal of Mathematical Neuroscience*, 10(1):15, September 2020.

[43] Eugene M. Izhikevich. *Dynamical Systems in Neuroscience*. MIT Press, 2007.

[44] Farzaneh Najafi, Gamaleldin F. Elsayed, Robin Cao, Eftychios Pnevmatikakis, Peter E. Latham, John P. Cunningham, and Anne K. Churchland. Excitatory and Inhibitory Subnetworks Are Equally Selective during Decision-Making and Emerge Simultaneously during Learning. *Neuron*, 105(1):165–179.e8, January 2020.

[45] Vincent S. C. Chien, Burkhard Maess, and Thomas R. Knösche. A generic deviance detection principle for cortical On/Off responses, omission response, and mismatch negativity. *Biol Cybern*, 113(5):475–494, December 2019.

[46] Xiao-Jing Wang. Neurophysiological and computational principles of cortical rhythms in cognition. 90(3):1195–1268.